

Structure and freezing of a fluid of long elongated molecules

This article has been downloaded from IOPscience. Please scroll down to see the full text article.

2004 J. Phys.: Condens. Matter 16 1695

(<http://iopscience.iop.org/0953-8984/16/10/002>)

View [the table of contents for this issue](#), or go to the [journal homepage](#) for more

Download details:

IP Address: 129.252.86.83

The article was downloaded on 27/05/2010 at 12:49

Please note that [terms and conditions apply](#).

Structure and freezing of a fluid of long elongated molecules

Pankaj Mishra, Jokhan Ram and Yashwant Singh

Department of Physics, Banaras Hindu University, Varanasi-221 005, India

Received 1 December 2003

Published 27 February 2004

Online at stacks.iop.org/JPhysCM/16/1695 (DOI: 10.1088/0953-8984/16/10/002)

Abstract

The pair correlation functions of a fluid of long elongated molecules interacting via the Gay–Berne pair potential are calculated using the Percus–Yevick integral equation theory. Numerical accuracy has been examined by considering a large number of spherical harmonic coefficients for each orientation-dependent functions for a system of molecules having a length-to-breadth ratio equal to 4.4 at different densities and temperatures. The pair correlation functions of the isotropic fluid found from the Percus–Yevick theory have been used in the density-functional theory to locate the isotropic–nematic, isotropic–smectic A and nematic–smectic A transitions. It is found that at low temperatures the fluid freezes directly into the smectic A phase on increasing the density. The nematic phase is found to stabilize in between the isotropic and smectic A phases only at high temperatures and high densities. The calculated phase diagram is in good qualitative agreement with computer simulation results.

1. Introduction

A system consisting of anisotropic molecules is known to exhibit liquid crystalline phases in between the isotropic liquid and the crystalline solid. The liquid crystalline phases that commonly occur in a system of long elongated molecules are nematic and smectic phases [1]. In the nematic phase the full translational symmetry of the isotropic fluid phase (denoted as R^3) is maintained, but the rotational symmetry $O(3)$ or $SO(3)$ (depending upon the presence or absence of the centre of symmetry) is broken. In the simplest form of the axially symmetric molecules the group $SO(3)$ (or $O(3)$) is replaced by one of the uniaxial symmetry $D_{\infty h}$ or D_{∞} . The phase possessing $R^3 \wedge D_{\infty h}$ (denoting the semi-direct product of the translational group R^3 and the rotational group $D_{\infty h}$) symmetry is known as the uniaxial nematic phase.

Smectic liquid crystals, in general, have a stratified structure with a long axis of molecules parallel to each other in layers. This situation corresponds to partial breakdown of translational invariance in addition to the breaking of the rotational invariance. Since a variety of molecular arrangements are possible within each layer, a number of smectic phases are possible. The simplest among them is the smectic A (SmA) phase. In this phase the centre of mass of

molecules in a layer are distributed as in a two dimensional fluid, but the molecular axes are on average along a direction normal to the smectic layer (i.e. the director $\hat{\mathbf{n}}$ is normal to the smectic layer). The symmetry of the SmA phase is $(R^2 \times Z) \wedge D_{\infty h}$ where R^2 corresponds to a two dimensional liquid structure and Z for a one dimensional periodic structure. The other non-chiral and non-tilted smectic phase seen in a system of long elongated molecules is the smectic B_h (SmB_h) phase. In each smectic layer of the SmB_h phase, the director is parallel to the layer normal as in the SmA phase, and there is short-range positional but long range bond-orientational hexagonal orders in the smectic plane. The azimuthally symmetrical x-ray ring of SmA is replaced by a six-fold modulated diffused pattern [2]. The phase is thus characterized by a D_{6h} point group symmetry and is uniaxial like SmA.

All these phases, including that of the isotropic liquid and the crystalline solids, are characterized by the average position and orientation of molecules and by the intermolecular spatial and orientational correlations. The factor responsible for the existence of these distinguishing features is the anisotropy in both the shape of the molecules and the attractive forces between them. The relationship between the intermolecular interactions and the relative stability of these phases is very intriguing and not yet fully understood. For a real system one faces the problem of knowing the accurate intermolecular interaction as a function of intermolecular separation and orientations. This is because the mesogenic molecules are so complex that none of the methods used to calculate interactions between molecules can be applied without drastic approximations. Consequently, one is forced to use phenomenological descriptions, either as a straightforward model unrelated to any particular physical system, or as a basis for a description by means of adjustable parameters between two molecules. Since our primary interest here is to relate the phases formed and their properties to the essential molecular factor responsible for the existence of liquid crystals, and not to calculate the properties of any real system, the use of the phenomenological potential is justified. One such phenomenological model which has attracted a lot of attention in computer simulations is the one proposed by Gay and Berne [3].

In the Gay–Berne (GB) pair potential model, the molecules are viewed as rigid units with axial symmetry. Each individual molecule i is represented by a centre-of-mass position \mathbf{r}_i and an orientational unit vector $\hat{\mathbf{e}}_i$ which is in the direction of the main symmetry axis of the molecule. The GB interaction energy between a pair of molecules (i, j) is given by

$$u(\mathbf{r}_{ij}, \hat{\mathbf{e}}_i, \hat{\mathbf{e}}_j) = 4\epsilon(\hat{\mathbf{e}}_i, \hat{\mathbf{e}}_j, \hat{\mathbf{r}}_{ij})(R^{-12} - R^{-6}) \quad (1.1)$$

where

$$R = \frac{r_{ij} - \sigma(\hat{\mathbf{e}}_i, \hat{\mathbf{e}}_j, \hat{\mathbf{r}}_{ij}) + \sigma_0}{\sigma_0}. \quad (1.2)$$

Here σ_0 is a constant defining the molecular diameter, r_{ij} is the distance between the centre of mass of molecules i and j and $\hat{\mathbf{r}}_{ij} = \mathbf{r}_{ij}/|\mathbf{r}_{ij}|$ is a unit vector along the centre–centre vector $\mathbf{r}_{ij} = \mathbf{r}_i - \mathbf{r}_j$. $\sigma(\hat{\mathbf{e}}_i, \hat{\mathbf{e}}_j, \hat{\mathbf{r}}_{ij})$ is the distance (for given molecular orientation) at which the intermolecular potential vanishes and is given by

$$\sigma(\hat{\mathbf{e}}_i, \hat{\mathbf{e}}_j, \hat{\mathbf{r}}_{ij}) = \sigma_0 \left[1 - \chi \left(\frac{(\hat{\mathbf{e}}_i \cdot \hat{\mathbf{r}}_{ij})^2 + (\hat{\mathbf{e}}_j \cdot \hat{\mathbf{r}}_{ij})^2 - 2\chi(\hat{\mathbf{e}}_i \cdot \hat{\mathbf{r}}_{ij})(\hat{\mathbf{e}}_j \cdot \hat{\mathbf{r}}_{ij})(\hat{\mathbf{e}}_i \cdot \hat{\mathbf{e}}_j)}{1 - \chi^2(\hat{\mathbf{e}}_i \cdot \hat{\mathbf{e}}_j)^2} \right) \right]^{-1/2}. \quad (1.3)$$

The parameter χ is a function of the ratio x_0 ($\equiv \sigma_e/\sigma_s$) which is defined in terms of the contact distances when the particles are end-to-end (e) and side-by-side (s),

$$\chi = \frac{x_0^2 - 1}{x_0^2 + 1}. \quad (1.4)$$

The orientational dependence of the potential well depth is given by a product of two functions

$$\epsilon(\hat{\mathbf{e}}_i, \hat{\mathbf{e}}_j, \hat{\mathbf{r}}_{ij}) = \epsilon_0 \epsilon^v(\hat{\mathbf{e}}_i, \hat{\mathbf{e}}_j) \epsilon^{\mu}(\hat{\mathbf{e}}_i, \hat{\mathbf{e}}_j, \hat{\mathbf{r}}_{ij}) \quad (1.5)$$

where the scaling parameter ϵ_0 is the well depth for the cross configuration ($\hat{\mathbf{e}}_i \cdot \hat{\mathbf{e}}_j = \hat{\mathbf{r}}_{ij} \cdot \hat{\mathbf{e}}_i = \hat{\mathbf{r}}_{ij} \cdot \hat{\mathbf{e}}_j = 0$). The first of these functions

$$\epsilon(\hat{\mathbf{e}}_i, \hat{\mathbf{e}}_j) = [1 - \chi^2(\hat{\mathbf{e}}_i \cdot \hat{\mathbf{e}}_j)^2]^{-1/2} \quad (1.6)$$

favours the parallel alignment of the particle and so aids liquid crystal formations. The second function has a form analogous to $\sigma(\hat{\mathbf{e}}_i, \hat{\mathbf{e}}_j, \hat{\mathbf{r}}_{ij})$, i.e.

$$\epsilon'(\hat{\mathbf{e}}_i, \hat{\mathbf{e}}_j, \hat{\mathbf{r}}_{ij}) = \left[1 - \chi' \left(\frac{(\hat{\mathbf{e}}_i \cdot \hat{\mathbf{r}}_{ij})^2 + (\hat{\mathbf{e}}_j \cdot \hat{\mathbf{r}}_{ij})^2 - 2\chi'(\hat{\mathbf{e}}_i \cdot \hat{\mathbf{r}}_{ij})(\hat{\mathbf{e}}_j \cdot \hat{\mathbf{r}}_{ij})(\hat{\mathbf{e}}_i \cdot \hat{\mathbf{e}}_j)}{1 - \chi'^2(\hat{\mathbf{e}}_i \cdot \hat{\mathbf{e}}_j)^2} \right) \right]. \quad (1.7)$$

The parameter χ' is determined by the ratio of the well depth as

$$\chi' = \frac{k'^{1/\mu} - 1}{k'^{1/\mu} + 1}. \quad (1.8)$$

Here k' is well-depth ratio for the side-by-side and end-to-end configuration.

The GB model contains four parameters (x_0, k', μ, ν) that determine the anisotropy in the repulsive and attractive forces in addition to two parameters (σ_0, ϵ_0) that scale the distance and energy, respectively. Though x_0 measures the anisotropy of the repulsive core, it also determines the difference in the depth of the attractive well between the side-by-side and the cross configurations. Both x_0 and k' play important role in stabilizing the liquid crystalline phases. The exact role of the other two parameters μ and ν are not very obvious; though they appear to affect the anisotropic attractive forces in a subtle way.

The phase diagram found for the system interacting via the GB potential of equations (1.1)–(1.8) exhibits isotropic, nematic and SmB phases [4, 5] for $x_0 = 3.0, k' = 5.0, \mu = 2$ and $\nu = 1$. An island of SmA is, however, found to appear in the phase diagram at a value of x_0 slightly greater than 3.0 [5]. The range of SmA extends to both higher and lower temperatures as x_0 is increased. Also as x_0 is increased, the isotropic–nematic (I–N) transition is seen to move to lower density (and pressure) at a given temperature. Bates and Luckhurst [6] have investigated the phases and phase transitions for the GB potential with $x_0 = 4.4, k' = 20.0, \mu = 1$ and $\nu = 1$ using the isothermal–isobaric Monte Carlo simulations. At low pressure they found isotropic, SmA and SmB phases but not the nematic phase. However as the pressure is increased, the nematic phase also becomes stabilized and a sequence of I–N–SmA and SmB was found.

In this paper we consider a fluid of long elongated molecules with length-to-breadth ratio, $x_0 = 4.4$, interacting via the Gay–Berne pair potential. In order to compare our results with those of the computer simulations we take the potential parameters to be the same as those given in [6]. The paper is organized as follows: in section 2, we describe the Percus–Yevick integral equation theory for the calculation of the pair correlation functions of the isotropic phase and compare our results with those found by simulations. In section 3 the density-functional formalism has been used to locate the freezing transitions and freezing parameters for the I–N, I–SmA and N–SmA transitions. The paper ends with a discussion given in section 4.

2. Isotropic phase: pair correlation functions

The structural information of an isotropic liquid is contained in the two particle density distribution $\rho(\mathbf{1}, \mathbf{2})$ as the single particle density distribution is constant independent of position and orientation. The two-particle density distribution $\rho(\mathbf{1}, \mathbf{2})$ measures the probability of finding simultaneously a molecule in a volume element $d\mathbf{r}_1 d\Omega_1$ centred at (\mathbf{r}_1, Ω_1) and a second molecule in a volume element $d\mathbf{r}_2 d\Omega_2$ at (\mathbf{r}_2, Ω_2) . The pair correlation function $g(\mathbf{1}, \mathbf{2})$ is related to $\rho(\mathbf{1}, \mathbf{2})$ as

$$g(\mathbf{1}, \mathbf{2}) = \frac{\rho(\mathbf{1}, \mathbf{2})}{\rho(\mathbf{1})\rho(\mathbf{2})} \quad (2.1)$$

where $\rho(\mathbf{i})$ is the single particle density distribution. Since for the isotropic fluid $\rho(\mathbf{1}) = \rho(\mathbf{2}) = \rho_f = \langle N \rangle / V$, where $\langle N \rangle$ is the average number of molecules in the volume V ,

$$\rho_f^2 g(\mathbf{r}, \Omega_1, \Omega_2) = \rho(\mathbf{r}, \Omega_1, \Omega_2) \quad (2.2)$$

where $\mathbf{r} = \mathbf{r}_2 - \mathbf{r}_1$. In the isotropic phase $\rho(\mathbf{1}, \mathbf{2})$ depends only on distance $|\mathbf{r}_2 - \mathbf{r}_1| = r$, the orientation of molecules with respect to each other and on the direction of vector \mathbf{r} .

The pair distribution function $g(\mathbf{1}, \mathbf{2})$ of the isotropic fluid is of particular interest as it is the lowest order microscopic quantity that contains information about the translational and orientational structures of the system and also has direct contact with intermolecular (as well as with intramolecular) interactions. For an ordered phase, on the other hand, as shown in the next section, most of the structural information is contained in the single particle distribution $\rho(\mathbf{1})$. In the density functional theory of freezing the single particle distribution $\rho(\mathbf{1})$ of an ordered phase is expressed in terms of the pair correlation function of the isotropic fluid (see section 3).

The value of $g(\mathbf{1}, \mathbf{2})$ as a function of intermolecular separation and orientation at a given temperature and density is found either by computer simulation or by solving the Ornstein–Zernike (OZ) equation

$$h(\mathbf{1}, \mathbf{2}) = c(\mathbf{1}, \mathbf{2}) + \rho_f \int c(\mathbf{1}, \mathbf{3})h(\mathbf{2}, \mathbf{3}) d\mathbf{3} \quad (2.3)$$

where $d\mathbf{3} = d\mathbf{r}_3 d\Omega_3$, and $h(\mathbf{1}, \mathbf{2}) = g(\mathbf{1}, \mathbf{2}) - 1$ and $c(\mathbf{1}, \mathbf{2})$ are, respectively, the total and direct pair correlation functions (DCF), using a suitable closure relation such as the Percus–Yevick (PY) integral equation, and hypernetted chain (HNC) relations. Approximations are introduced through these closure relations [7].

The Percus–Yevick closure relation is written in various equivalent forms. The form adopted here is

$$c^{\text{PY}}(\mathbf{1}, \mathbf{2}) = f(\mathbf{1}, \mathbf{2})[g(\mathbf{1}, \mathbf{2}) - c(\mathbf{1}, \mathbf{2})] \quad (2.4)$$

where $f(\mathbf{1}, \mathbf{2}) = \exp[-\beta u(\mathbf{1}, \mathbf{2})] - 1$ is the Mayer function, $\beta = (k_B T)^{-1}$ and $u(\mathbf{1}, \mathbf{2})$ is a pair potential of interaction. Since for the isotropic liquid DCF is an invariant pair wise function, it has an expansion in body fixed (BF) frame in terms of basic set of rotational invariants, as

$$c(\mathbf{r}_{12}, \Omega_1, \Omega_2) = \sum_{l_1 l_2 m} c_{l_1 l_2 m}(r_{12}) Y_{l_1 m}(\Omega_1) Y_{l_2 \underline{m}}(\Omega_2) \quad (2.5)$$

where $\underline{m} = -m$. The coefficients $c_{l_1 l_2 m}(r_{12})$ are defined as

$$c_{l_1 l_2 m}(r_{12}) = \int c(\mathbf{r}_{12}, \Omega_1, \Omega_2) Y_{l_1 m}^*(\Omega_1) Y_{l_2 \underline{m}}^*(\Omega_2) d\Omega_1 d\Omega_2. \quad (2.6)$$

Expanding all the angle dependent functions in BF frame, the OZ equation reduces to a set of algebraic equation in Fourier space

$$h_{l_1 l_2 m}(k) = c_{l_1 l_2 m}(k) + (-1)^m \frac{\rho_f}{4\pi} \sum_{l_3} c_{l_1 l_3 m}(k) h_{l_3 l_2 m}(k) \quad (2.7)$$

where the summation is over allowed values of l_3 . The PY closure relation is expanded in spherical harmonics in the body (or space) fixed frame. The pair correlation functions are then found by solving these self-consistently [8].

In our earlier work [9, 10] we considered 30 harmonics in expansion of each orientation dependent function (see equation (2.5)), i.e. the series were truncated at a value of l indices equal to 6. Since the accuracy of the results depends on this number and as the anisotropy of the shape taken here is larger than the earlier work, we considered 54 harmonics. The series of each orientation dependent function was truncated at the value of l indices equal to 8. The

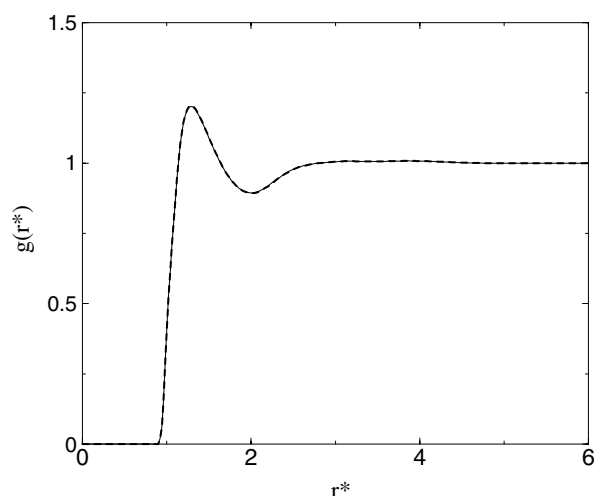


Figure 1. Pair-correlation functions of the centre of mass $g(r^*)$ for GB fluid with parameters $x_0 = 4.4$, $k' = 20.0$, $\mu = 1$ and $\nu = 1$, at $\eta = 0.44$ and $T^* = 1.40$. The solid and dashed curves are, respectively, for 30 and 54 body-fixed harmonic coefficients. These two curves are indistinguishable on the scale of the figure.

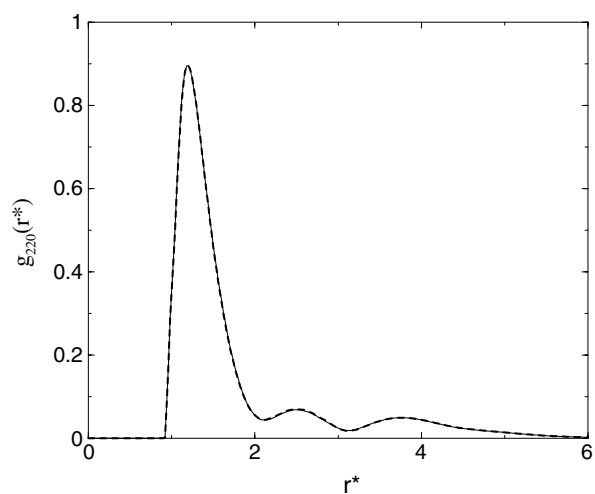


Figure 2. Spherical harmonic coefficient $g_{220}(r^*)$ in the body-fixed frame. The curves are the same as in figure 1.

numerical procedure for solving equation (2.7) along with the PY closer relation is the same as discussed in [10].

In figure 1 we compare the values of $g(r^*) = 1 + h_{000}(r^*)/4\pi$ in the BF frame having 30 and 54 harmonic coefficients at $T^* (=k_B T/\epsilon_0) = 1.40$ and density $\eta (= \pi \rho_f \sigma_0^3 x_0/6) = 0.44$ for $x_0 = 4.4$, where $r^* = r/\sigma_0$ is the reduced interparticle separation. One other projection of the pair correlation, $g_{220}(r^*)$, is shown in figure 2 for the same set of parameters. It is obvious from these figures that even for fairly long molecules one gets good results with 30 harmonics. We therefore conclude that any error in the correlation functions evaluated using the integral equations described above is not due to truncation of series.

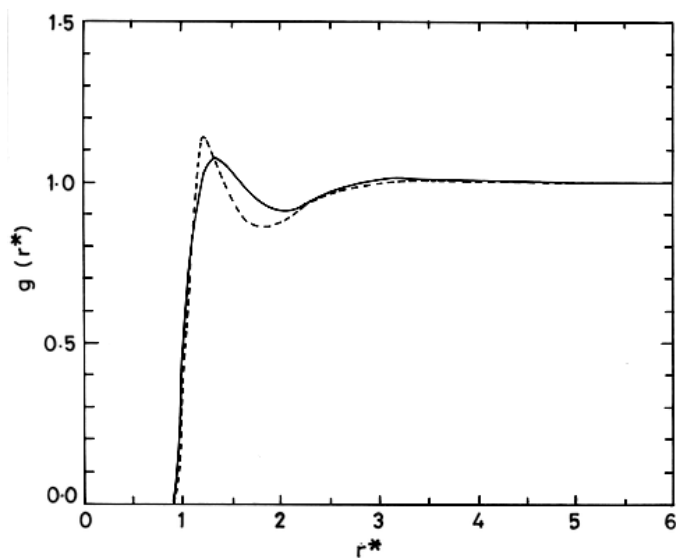


Figure 3. Pair-correlation function of the centre of mass $g(r^*)$ for GB fluid with parameters $x_0 = 4.4$, $k' = 20.0$, $\mu = 1$ and $\nu = 1$ at $\eta = 0.36$ and $T^* = 1.80$. The solid curve is our PY result and the dashed curve is the simulation result of Bates and Luckhurst [6].

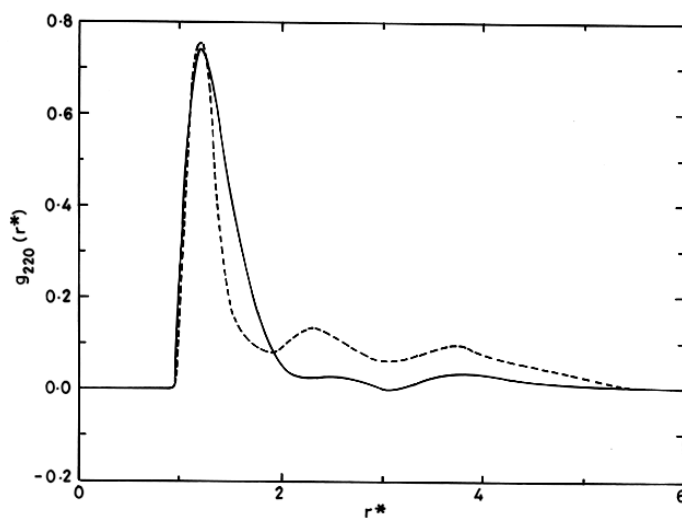


Figure 4. Spherical harmonic coefficient $g_{220}(r^*)$ in the body-fixed frame. The curves are the same as in figure 3.

In figures 3 and 4 we compare the values of $g(r^*)$ and $g_{220}(r^*)$, respectively, with those obtained by computer simulations [6] for $\eta = 0.36$ and $T^* = 1.80$. The PY peak in $g(r^*)$ (see figure 3) is broad and of less height than one found from the simulation. This indicates that the PY theory is unable to predict the correct orientational correlations in neighbouring molecules. The fact that the peak in g_{220} is broad and oscillations at large r^* decay faster than those found in simulation further indicates that the PY theory underestimates the orientational correlations present in the isotropic phase.

3. Freezing transitions

In the density functional approach one uses the grand thermodynamic potential defined as

$$-W = \beta A - \beta \mu_c \int d\mathbf{x} \rho(\mathbf{x}) \quad (3.1)$$

where A is the Helmholtz free energy, μ_c the chemical potential and $\rho(\mathbf{x})$ is a singlet distribution function to locate the transition. It is convenient to subtract the isotropic fluid thermodynamic potential from W and write it as [11]

$$\Delta W = W - W_f = \Delta W_1 + \Delta W_2 \quad (3.2)$$

with

$$\frac{\Delta W_1}{N} = \frac{1}{\rho_f V} \int d\mathbf{r} d\Omega \left\{ \rho(\mathbf{r}, \Omega) \ln \left[\frac{\rho(\mathbf{r}, \Omega)}{\rho_f} \right] - \Delta \rho(\mathbf{r}, \Omega) \right\} \quad (3.3)$$

and

$$\frac{\Delta W_2}{N} = -\frac{1}{2\rho_f} \int d\mathbf{r}_{12} d\Omega_1 d\Omega_2 \Delta \rho(\mathbf{r}_1, \Omega_1) c(\mathbf{r}_{12}, \Omega_1, \Omega_2) \Delta \rho(\mathbf{r}_2, \Omega_2). \quad (3.4)$$

Here $\Delta \rho(\mathbf{x}) = \rho(\mathbf{x}) - \rho_f$, where ρ_f is the density of the coexisting liquid.

The minimization of ΔW with respect to arbitrary variation in the ordered phase density subject to a constraint that corresponds to some specific feature of the ordered phase leads to

$$\ln \frac{\rho(\mathbf{r}_1, \Omega_1)}{\rho_f} = \lambda_L + \int d\mathbf{r}_2 d\Omega_2 c(\mathbf{r}_{12}, \Omega_1, \Omega_2; \rho_f) \Delta \rho(\mathbf{r}_2, \Omega_2) \quad (3.5)$$

where λ_L is Lagrange multiplier which appears in the equation because of constraint imposed on the minimization.

Equation (3.5) is solved by expanding the singlet distribution $\rho(\mathbf{x})$ in terms of the order parameters that characterize the ordered structures. One can use the Fourier series and Wigner rotation matrices to expand $\rho(\mathbf{r}, \Omega)$. Thus

$$\rho(\mathbf{r}, \Omega) = \rho_0 \sum_q \sum_{lmn} Q_{lmn}(G_q) \exp(i\mathbf{G}_q \cdot \mathbf{r}) D_{mn}^l(\Omega) \quad (3.6)$$

where the expansion coefficients

$$Q_{lmn}(G_q) = \frac{2l+1}{N} \int d\mathbf{r} \int d\Omega \rho(\mathbf{r}, \Omega) \exp(-i\mathbf{G}_q \cdot \mathbf{r}) D_{mn}^{*l}(\Omega) \quad (3.7)$$

are the order parameters, \mathbf{G}_q the reciprocal lattice vectors, ρ_0 the mean number density of the ordered phase and $D_{mn}^{*l}(\Omega)$ the generalized spherical harmonics or Wigner rotation matrices. Note that for a uniaxial system consisting of cylindrically symmetric molecules $m = n = 0$ and, therefore, one has

$$\rho(\mathbf{r}, \Omega) = \rho_0 \sum_l \sum_q Q_{lq} \exp(i\mathbf{G}_q \cdot \mathbf{r}) P_l(\cos \theta) \quad (3.8)$$

and

$$Q_{lq} = \frac{2l+1}{N} \int d\mathbf{r} \int d\Omega \rho(\mathbf{r}, \Omega) \exp(-i\mathbf{G}_q \cdot \mathbf{r}) P_l(\cos \theta) \quad (3.9)$$

where $P_l(\cos \theta)$ is the Legendre polynomial of degree l and θ is the angle between the cylindrical axis of a molecule and the director.

In the present calculation we consider two orientational order parameters

$$\bar{P}_l = \frac{Q_{l0}}{2l+1} = \langle P_l(\cos \theta) \rangle \quad (3.10)$$

with $l = 2$ and 4 , one order parameter corresponding to positional order along the Z axis,

$$\bar{\mu} = Q_{00}(G_z) = \left\langle \cos\left(\frac{2\pi}{d}z\right) \right\rangle \quad (3.11)$$

(d , being the layer spacing) and one mixed order parameter that measures the coupling between the positional and orientational ordering and is defined as,

$$\tau = \frac{1}{5} Q_{20}(G_z) = \left\langle \cos\left(\frac{2\pi}{d}z\right) P_l(\cos\theta) \right\rangle. \quad (3.12)$$

The angular brackets in the above equations indicate the ensemble average.

The following order parameter equations are obtained by using equations (3.5)–(3.9):

$$\bar{P}_l = \frac{1}{2d} \int_0^d dz_1 \int_0^\pi \sin\theta_1 d\theta_1 P_l(\cos\theta_1) \exp[\text{sum}] \quad (3.13)$$

$$\bar{\mu} = \frac{1}{2d} \int_0^d dz_1 \int_0^\pi \sin\theta_1 d\theta_1 \cos\left(\frac{2\pi z_1}{d}\right) \exp[\text{sum}] \quad (3.14)$$

$$\tau = \frac{1}{2d} \int_0^d dz_1 \int_0^\pi \sin\theta_1 d\theta_1 P_2(\cos\theta_1) \cos\left(\frac{2\pi z_1}{d}\right) \exp[\text{sum}] \quad (3.15)$$

and the change in density at the transition is found from the relation

$$1 + \Delta\rho^* = \frac{1}{2d} \int_0^d dz_1 \int_0^\pi \sin\theta_1 d\theta_1 \exp[\text{sum}]. \quad (3.16)$$

Here

$$\text{sum} = \Delta\rho^* \hat{C}_{00}^0 + 2\bar{\mu} \cos\left(\frac{2\pi z}{d}\right) \hat{C}_{00}^1(\theta_1) + \bar{P}_2 \hat{C}_{20}^0(\theta_1) + \bar{P}_4 \hat{C}_{40}^0(\theta_1) + 2\tau \cos\left(\frac{2\pi z}{d}\right) \hat{C}_{20}^1(\theta_1) \quad (3.17)$$

and

$$\begin{aligned} \hat{C}_{L0}^q(\theta_1) &= \left(\frac{2l+1}{4\pi}\right)^{1/2} \rho_f \sum_{l_1 l} i^l (2l_1+1)^{1/2} (2l+1)^{1/2} C_g(l_1 L l; 000) P_{l_1}(\cos\theta_1) \\ &\times \int_0^\infty c_{l_1 L l}(r_{12}) j_l(G_q r_{12}) r_{12}^2 dr_{12} \end{aligned} \quad (3.18)$$

where $C_g(l_1 L l; 000)$ are the Clebsch–Gordan coefficients and $G_q = 2\pi/d$.

In the isotropic phase all the four order parameters become zero. In the nematic phase the orientational order parameters \bar{P}_2 and \bar{P}_4 become non-zero but the other two parameters $\bar{\mu}$ and τ remain zero. This is because the nematic phase has no long range positional order. In the SmA phase all four order parameters are non-zero showing that the system has both long range orientational and positional order along one direction. Equations (3.13)–(3.16) are solved self-consistently using the values of the direct pair correlation function harmonics $c_{l_1 l_2 l}(r)$ evaluated at a given value of T^* and η as described in the previous section. This calculation is repeated with different values of d , the interlayer spacing. By substituting these solutions in equations (3.2)–(3.4) we find the grand thermodynamic potential difference between ordered and isotropic phases, i.e.

$$-\frac{\Delta W}{N} = -\Delta\rho^* + \frac{1}{2} \Delta\rho^* (2 + \Delta\rho^*) \hat{C}_{00}^0 + \frac{1}{2} (\bar{P}_2^2 \hat{C}_{22}^0 + \bar{P}_4^2 \hat{C}_{44}^0) + \bar{\mu}^2 \hat{C}_{00}^1 + 2\bar{\mu}\tau \hat{C}_{20}^1 + \tau^2 \hat{C}_{22}^1 \quad (3.19)$$

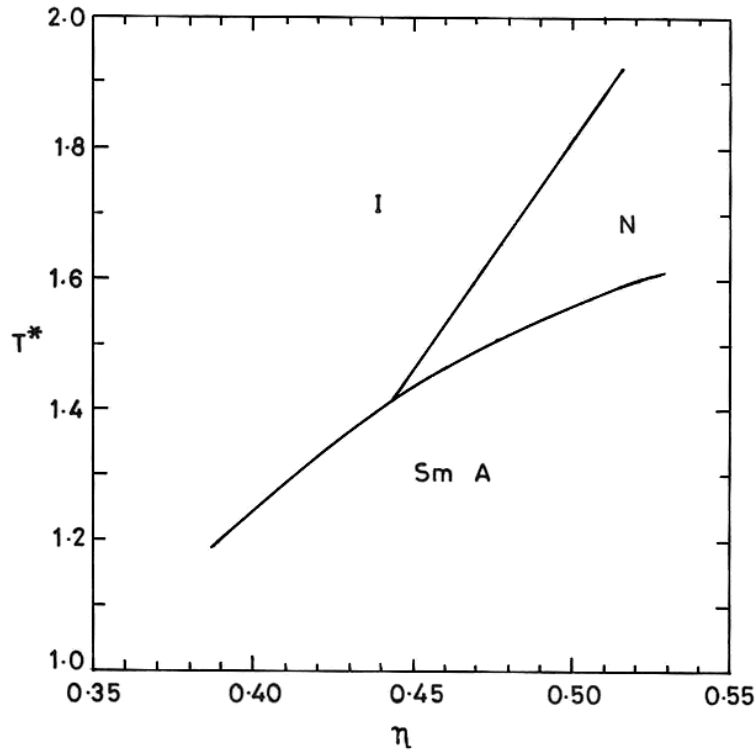


Figure 5. Phase diagram for the GB potential with parameters $x_0 = 4.4$, $k' = 20.0$, $\mu = 1$ and $\nu = 1$ using the density-functional theory.

where

$$\hat{C}_{LL'}^q = (2L+1)^{1/2}(2L'+1)^{1/2}\rho_f \sum_l i^l \left(\frac{2l+1}{4\pi}\right)^{1/2} C_g(LL'l; 000) \times \int_0^\infty c_{LL'l}(r_{12}) j_l(G_q r_{12}) r_{12}^2 dr_{12}. \quad (3.20)$$

At a given temperature and density a phase with the lowest grand potential is taken as the stable phase. Phase coexistence occurs at the values of ρ_f that makes $-\Delta W/N = 0$ for the ordered and the liquid phases. The transition from nematic to the SmA is determined by comparing the values of $-\Delta W/N$ of these two phases at a given temperature and at different densities. The value of the interlayer spacing d , is found by minimizing the grand potential with respect to d . After selecting the value of d for a given density and temperature we locate the transition point using the procedure outlined above. Our results are summarized in table 1 and figure 5. We see that at low temperatures, i.e. at $T^* = 1.2$ and 1.4 the isotropic liquid freezes directly into SmA on increasing the density. Nematic phase is not stable at these temperatures. However, at $T^* = 1.6$ the isotropic liquid on increasing the density is found first to freeze into the nematic phase at $\eta = 0.49$ and on further increasing the density the nematic phase transforms into the SmA phase at $\eta = 0.519$. At high temperature, $T^* = 1.8$ the transition is found to take place between the isotropic and nematic only for the density range considered by us.

Using the results summarized in table 1 we draw the phase diagram in figure 5 in the density-temperature plane.

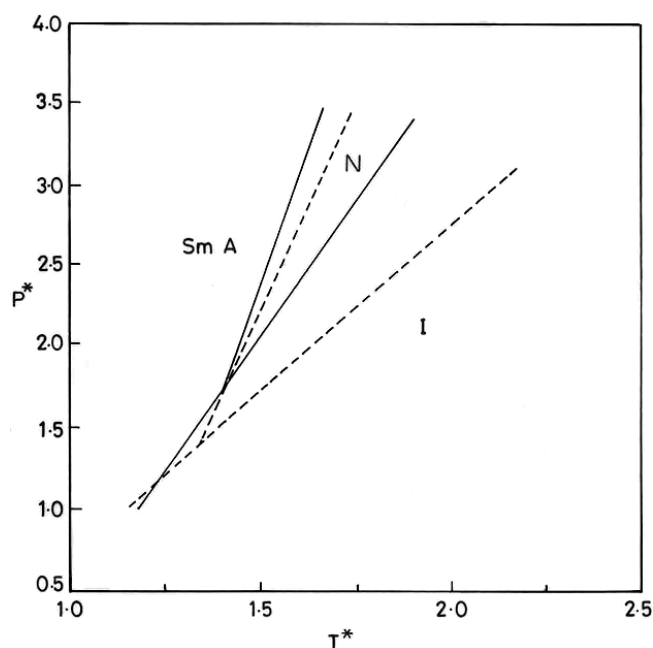


Figure 6. Phase diagram for the GB potential with parameters $x_0 = 4.4$, $k' = 20.0$, $\mu = 1$ and $\nu = 1$. The solid lines indicate the phase boundaries obtained by using the density-functional theory while dashed lines are the simulation results of Bates and Luckhurst [6].

Table 1. Values of the order parameters at the transitions for the GB potential with $x_0 = 4.4$, $k' = 20$, $\mu = \nu = 1$. Quantities in reduced units are $d^* = d/\sigma_0$, pressure $P^* = P\sigma_0^3/\epsilon_0$, $\mu_c^* = \mu_c/\epsilon_0$, and $\eta = \pi\rho_f\sigma_0^3x_0/6$.

T^*	Transition	η	d^*	$\Delta\rho^*$	$\bar{\mu}$	\bar{P}_2	\bar{P}_4	τ	P^*	μ_c^*
1.20	I-SmA	0.386	3.69	0.214	0.66	0.99	0.70	0.54	1.05	6.61
1.40	I-SmA	0.439	3.90	0.164	0.65	0.95	0.62	0.53	1.71	11.38
1.60	I-N	0.471	0.0	0.042	0.0	0.59	0.35	0.0	2.38	14.37
	N-SmA	0.519	3.98	0.016	0.46	0.94	0.67	0.39	3.01	17.34
1.80	I-N	0.498	0.0	0.038	0.0	0.61	0.35	0.0	3.10	18.41

4. Discussions

The phase diagram shown in figure 5 is in good qualitative agreement with the one found by computer simulations [6]. At low temperature the nematic is unstable; on increasing the density the fluid freezes directly into the SmA phase. The nematic phase is found to stabilize in between the isotropic and SmA phases only for $T^* \geq 1.5$. The quantitative agreement shown in figure 6 in the temperature–pressure plane is, however, not so encouraging.

At a given temperature the I–N transition is found to take place at higher pressure (or density) compared to that of simulation results. The gap seems to increase with the temperature. Though a similar feature is seen in the N–SmA transition, the gap in this case is small compared to that of the I–N transition. The region of existence of the nematic phase in the T – P plane (or T – η plane) is therefore narrower than that reported in [6]. This is also reflected in the ratio of N–SmA and I–N transition temperatures, T_{N-A}/T_{I-N} . For example, at $P^* = 3.0$ we

find $T_{N-A}/T_{I-N} = 0.890$, whereas the value reported in [6] is 0.795. For all the temperatures studied by us we found the N–SmA transition to be of first order. The values of the order parameters and the change in density at the transition are also found to be higher than those given in [6]. For example, the change in the density for the I–SmA transition at $T^* = 1.2$ is found to be 21.4% while the value given by Bates and Luckhurst [6] at $T^* = 1.15 \pm 0.05$ is 15.9%. The orientational order parameter P_2 at the I–N transition is found to be close to 0.60 whereas in [6] its value is close to 0.45.

All these features can easily be understood from the fact that the transitions at a given temperature in our calculation take place at higher densities than those found in simulations. As has already been pointed out in section 2, the PY theory underestimates the orientational correlations. Therefore the critical correlations at which the isotropic fluid becomes unstable is found to be higher compared to the actual value. This deficiency of the PY theory is found to increase with increasing temperature. This also explains why in figure 6 the I–N transition boundary is relatively more displaced than the N–SmA boundary. It is therefore necessary to find the correlations in the isotropic phase more accurately than those given by the PY theory.

Acknowledgment

The work was supported by the Department of Science and Technology (India) through a project grant.

References

- [1] de Gennes P G and Prost J 1993 *The Physics of Liquid Crystals* (Oxford: Clarendon)
- Chandrasekher S 1977 *Liquid Crystals* (London: Cambridge University Press)
- Collings P J and Patel J S (ed) 1997 *Handbook of Liquid Crystal Research* (New York: Oxford University Press)
- [2] Pindak R, Moncton D E, Davey S C and Goodby J W 1981 *Phys. Rev. Lett.* **46** 1135
- [3] Gay J G and Berne B J 1981 *J. Chem. Phys.* **74** 3316
- [4] Miguel E D, Rull L F, Chalam M K and Gubbins K E 1991 *Mol. Phys.* **74** 405
- [5] Brown J T, Allen M P, Martin del Rio E and Miguel E D 1998 *Phys. Rev. E* **57** 6685
- [6] Bates M A and Luckhurst G R 1999 *J. Chem. Phys.* **110** 7087
- [7] Gray C G and Gubbins K E 1984 *Theory of Molecular Fluids* vol 1 (Oxford: Clarendon)
- [8] Ram J and Singh Y 1991 *Phys. Rev. A* **44** 3718
- Ram J, Singh R C and Singh Y 1994 *Phys. Rev. E* **49** 5117
- [9] Singh R C, Ram J and Singh Y 1996 *Phys. Rev. E* **54** 977
- [10] Singh R C, Ram J and Singh Y 2002 *Phys. Rev. E* **65** 031711
- [11] Singh Y 1991 *Phys. Rep.* **207** 351